Towards electrical detection of plasmons in all-silicon pin-diodes

Inga A. Fischer[*,1], **Jyh-Lih Wu**[2], **Ralf Vogelgesang**[**,2], **and Jörg Schulze**[1]

[1] Institut für Halbleitertechnik, Universität Stuttgart, Pfaffenwaldring 47, 70569 Stuttgart, Germany
[2] Max Planck Institut für Festkörperforschung, Heisenbergstraße 1, 70569 Stuttgart, Germany

[*] Corresponding author: e-mail fischer@iht.uni-stuttgart.de, Phone: +49 711 685 68006, Fax: +49 711 685 68044
[**] e-mail r.vogelgesang@fkf.mpg.de, Phone: +49 711 689 1581, Fax: +49 711 689 1662

We investigate the possibility for optically exciting and electrically detecting surface plasmon polaritons (SPPs) in a set-up fully compatible with complementary-metal-oxide-semiconductor that consists of a silicon pin-diode. A grating in the aluminum electrode of the pin-diode is intended to enable the optical excitation of SPPs at the interface between the aluminum metallization and the SiO_2-passivation of the diode. When the SPP propagates towards the pin-diode and excites electron–hole pairs, it can be detected on the basis of the resulting photocurrent. We report on preliminary results obtained with scanning photocurrent microscopy with three different laser wavelengths (458, 512, and 633 nm).

1 Introduction The continuous downscaling of transistor dimension has been the driving force behind device performance increase for the last decades. However, the devices themselves as well as their metallic interconnects face increasing problems that have their origin in this very size reduction. Metallic interconnects in particular exhibit increasing delay times as well as power dissipation as they are scaled down; their performance is expected to be the limiting factor in further increasing overall device performance in approximately 10 years [1, 2]. Alternative concepts are, therefore, being explored.

In view of electronic operating frequencies approaching the terahertz and optical range, research is already underway that aims at translating electronic circuit elements into equivalent optical devices [3–5]. While optical circuitry may still be a somewhat far-fetched goal, optical information exchange between remote computers has long been a mature part of telecommunication technology. Current research and development is focusing on shorter-distance inter- and on-board communication via optical waveguides and transmission lines. Interestingly, as distances shrink, there is a trend away from purely photonic (dielectric) waveguides. For the increasingly short distances, the introduction of plasmonic transmission lines [6] has a number of advantages. Plasmonic waveguides are based on information transmission via surface plasmon polaritons (SPPs) and can, in

principle, be scaled down to the sub-100-nm regime [7]. This promises extremely high packing densities for the millimeter range in main board-to-chip and intra-chip information exchange, not achievable by photonic waveguides.

SPPs are electromagnetic excitations that propagate along the interface between a metal and a dielectric and are subject to attenuation due to dissipation in the metal. Therefore, SPPs have a finite propagation length, and moreover, tighter lateral confinement leads to increased absorption losses such that decreased waveguide sizes for plasmonic transmission lines come at the expense of increased energy dissipation. A thorough analysis comparing conventional, metallic interconnects to plasmonic interconnects has e.g. been performed in Ref. [8].

While plasmonic interconnects are clearly not suited for long-distance communication (beyond the centimeter range), where nearly loss-less photonic communication is preferable, they are excellent candidates for connecting a possible 'global' photonic interconnect layer that e.g. addresses off-chip information transmission to a conventional "local" interconnect level that handles the transmission of on-chip information [8]. As a prerequisite for this intermediate interconnect layer, the efficient optical generation of SPPs, their transmission over the required distances via waveguides as well as their electrical detection have to be realized. Moreover, for any plasmonic interconnects

considered for complementary metal-oxide-semiconductor (CMOS)-compatible device processing, SPP transmission and detection have to be implemented in CMOS compatible material systems. So far, passive elements of a transmission line in the form of CMOS-integrable plasmonic waveguides based on silicon have been proposed and experimentally realized [9–12]. Active elements for the silicon-based electrical generation of SPP signals [13], their modulation [14] as well as their conversion to electrical signals by means of germanium nanowires [15] have also been demonstrated. Further work, however, towards the realization of a fully CMOS-compatible transmission line is required.

In this paper, we present results on the fabrication of gratings for plasmon injection at aluminum–SiO_2 interfaces of the metallization–passivation layer of silicon pin-diodes as well as device characterizations with scanning photo-current microscopy (SPCM) under ambient conditions. In this measurement set-up, the current through the diode can be measured *in situ* under illumination with light of different wavelengths that is focused by means of a confocal optical microscope. Before reducing feature size to the nanoscale, our aim is to investigate how a set-up for the optical excitation and the electrical detection of SPPs can be realized in a conventional silicon pin-diode well within the micrometer range. While other types of metallization might be preferable for their plasmonic properties, aluminum has the advantage that it is fully CMOS-compatible.

2 Experimental set-up

2.1 Silicon pin-diode device fabrication process
Device fabrication starts with the layer growth of the vertical silicon pin-diode by means of molecular beam epitaxy (MBE). A double mesa etching process is used to form a n^+i-mesa on top of a p^+ buried layer. A schematic cutaway image is shown in Fig. 1.

The mesa diameter of the finished pin-diode varies between 1.5 and 80 μm. The mesa is subsequently passivated by depositing 300 nm of SiO_2 in a plasma-enhanced chemical vapour deposition (PECVD) process. In this passivation layer, contact holes are etched with a dry-etching process in a reactive ion etching (RIE) system; afterwards, 1.6 μm of aluminum as the final metallization layer is deposited by means of a sputtering process. This
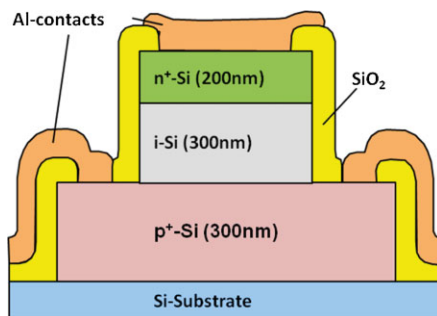

Figure 1 (online colour at: www.pss-b.com) Schematic cutaway image of the MBE layer stack of the finished silicon pin-diode.
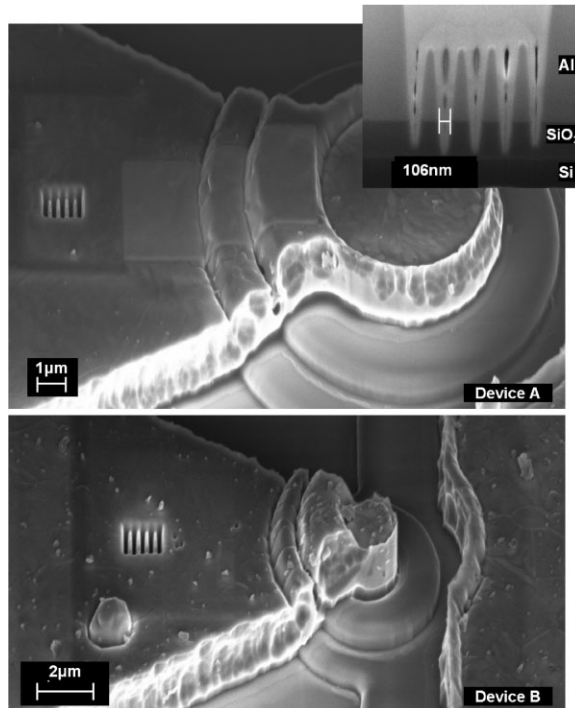

Figure 2 SEM images of the finished devices (device A shown above, device B shown below) with a grating incorporated in the aluminum contact leading up the diode double mesa. The inset shows the cutaway image of a similar grating structure, which has been filled in for better image contrast.

choice of aluminum thickness is made so as to guarantee coverage of the mesa sidewalls. As can be seen from scanning electron microscope (SEM) images in Fig. 2, the aluminum surface obtained from the sputtering process is not completely level but contains a number of sharp protrusions. In a final step, aluminum contacts to the top of the n^+i-mesa as well as to the p^+ buried layer are structured by means of a HCl/HBr dry etching process in an inductive coupled plasma RIE (ICP-RIE) system.

2.2 Fabrication of gratings for plasmon injection
Two of the pin-diodes with mesa diameters of 5 μm (device A) and 2 μm (device B) were then selected for further processing. A grating with the aim towards exciting SPPs at the interface between the aluminum- and the SiO_2-layer was structured by focused ion beam (FIB) milling in the aluminum contact layer. Figure 2 shows SEM images of the positions of the gratings with respect to the diode mesa for each of the two diodes, the SEM image of the cross section of a similar grating is shown in the inset of Fig. 2. As can be seen, the thickness of the aluminum layer makes the milling of a grating with 90° ridge sidewalls difficult to achieve. A lattice constant of approximately 200 nm can be assumed for each of the gratings at the aluminum–SiO_2 interface. The overall dimensions of each of the gratings are approximately 1 μm in width and 1.3 μm in length. In device A, the grating is situated at a distance of approximately 6 μm from the

Original

Paper

Phys. Status Solidi B **249**, No. 4 (2012)   775

upper mesa that contains the intrinsic region; in device B, grating and upper mesa are spaced approximately 4 μm apart.

If SPPs can be excited optically by illuminating the grating, they can propagate along the aluminum-SiO$_2$ interface. If they impinge on the silicon mesa, they can excite electron–hole pairs that are separated by the intrinsic field of the pin-structure, which generates a measurable photocurrent.

3 Device characterization and measurement results Figure 3 shows current–voltage characteristics of the two diodes in the absence of optical excitation. In order to investigate possible SPP excitations in the system, the devices were characterized with SPCM [16] under ambient conditions, using three different laser sources (of wavelengths 458, 514, and 633 nm). SPCM measurements were taken at zero and reverse bias of the pin-diodes.

Figures 4 and 5 show photocurrent maps of the grating area of device B at different laser illumination wavelengths and orientations of the polarization (Fig. 4) as well as different external bias conditions of the pin-diode (Fig. 5). In the photocurrent maps shown in Fig. 4, a clear photocurrent signal from the grating structure in the aluminum contact layer can be observed. The positions of the additional spot-like photocurrent peaks in proximity to the grating coincide with the protrusions in the aluminum metallization that originate from the deposition process, as can be inferred from Fig. 2.

A comparison of the photocurrent maps at the same light wavelength but for light polarized perpendicular and parallel to the ridges of the grating shows that the photocurrent signal is significantly stronger (by approximately a factor of three) for light polarized perpendicular to the ridges of the grating, as can be expected for plasmonic coupling structures [17]. The magnitude of the photoresponse increases with applied external bias, as shown in Fig. 5.

While plasmonic excitations could be at the origin of the photocurrent signals, other effects could also contribute. We therefore scanned a larger section of the device area, the
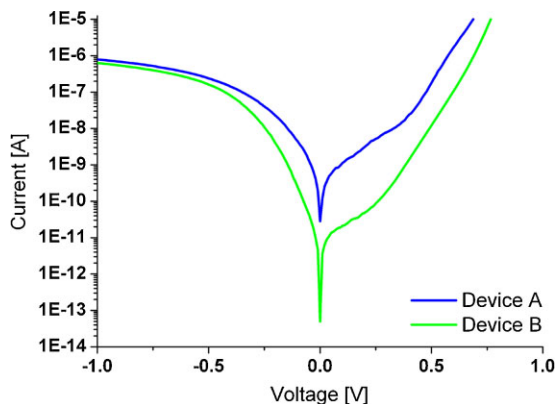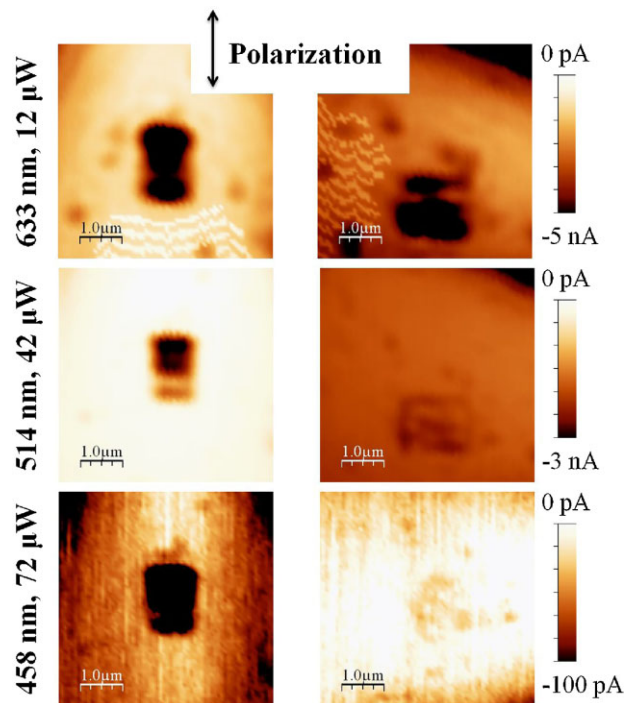

Figure 4 (online colour at: www.pss-b.com) Photocurrent maps of the grating of device B at different laser wavelengths and laser power. Laser polarization is perpendicular (left column) and parallel (right column) to the grating. All maps were taken at an external bias of −0.5 V.

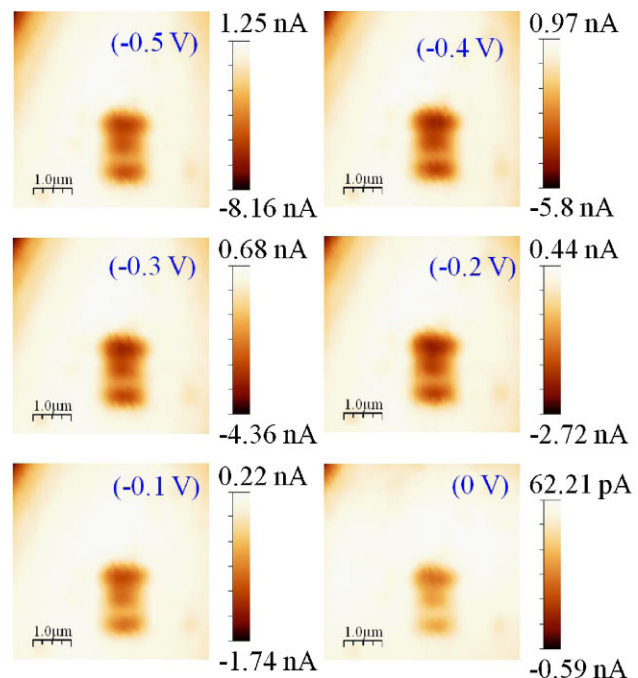**Figure 3** (online colour at: www.pss-b.com) Current–voltage characteristics of the devices.

Figure 5 (online colour at: www.pss-b.com) Bias dependence of the photocurrent maps of device B at a laser wavelength of 633 nm, 12 μW incident laser power and light polarization perpendicular to the grating.
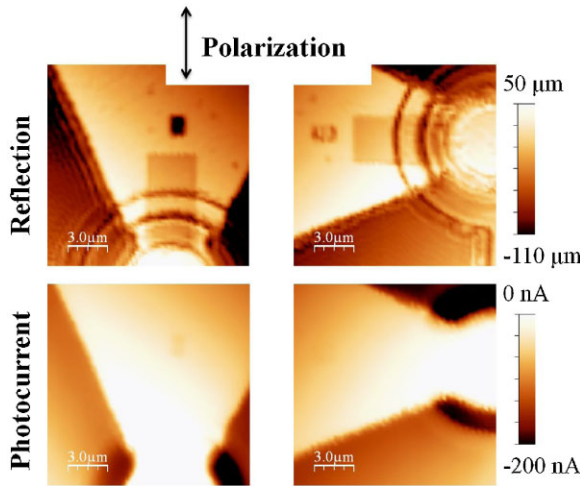
Figure 6 (online colour at: www.pss-b.com) Reflection images (upper row) and photocurrent maps (lower row) of device A at external bias of $-0.5\,V$ and with a laser wavelength of 633 nm. We observe a finite photocurrent from light directly impinging on the silicon substrate.

resulting photocurrent maps as well as reflection images of device A are shown in Fig. 6. Since the double mesa as the active region of the device is included in the scanning image, the largest photocurrent is observed when laser light impinges directly on the silicon mesa, irrespective of the polarization of the incident laser light. For light polarized perpendicular to the grating, a photocurrent peak that coincides with the position of the grating is also visible. However, we can also observe that a clear photocurrent signal is obtained from the regions where the laser light hits the silicon substrate, which is only covered by the transparent SiO_2 passivation layer in this area. As can be seen in Fig. 7, this photocurrent signal can be made to vanish with positive applied bias. However, at these bias conditions the signal from the grating coupler is also extenuated.

4 Discussion We can estimate the complex wavevectors k_{SPP} and the propagation lengths L_{SPP} of the SPPs that are excited at the different illumination wavelengths (458, 514, and 633 nm with corresponding vacuum wavevector
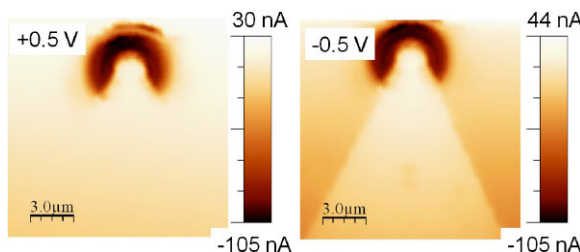

Figure 7 (online colour at: www.pss-b.com) Photocurrent maps of device B at a laser wavelength of 633 nm and with light polarization perpendicular to the grating.

Table 1 SPP wave vectors and propagation lengths at the aluminum–SiO_2 interface for the different laser wavelengths λ_{laser} used in the measurements.

λ_{laser} (nm)	Re(k_{SPP}) (1/μm)	L_{SPP} (μm)
458	20.8	2.48
514	18.4	3.22
633	14.7	4.49

$k_0 = 2\pi/\lambda_0$ according to

$$k_{SPP} = k_0 \sqrt{\frac{\varepsilon_{Al}\varepsilon_{SiO_2}}{\varepsilon_{Al} + \varepsilon_{SiO_2}}}, \tag{1}$$

and

$$L_{SPP} = \frac{1}{2\text{Im}(k_{SPP})}, \tag{2}$$

where ε_{SiO_2} and ε_{Al} are the permittivities of SiO_2 and aluminum, respectively [18, 19]. An SPP that is excited at the grating structure and subsequently travels along the aluminum–SiO_2 interface is theoretically able to reach the double mesa that contains the active layers but will have experienced significant damping according to the results given in Table 1. Moreover, these figures most likely overestimate the propagation length for SPPs in our device since the polycrystallinity of the sputtered aluminum metallization layer can be expected to induce additional propagation losses. This might explain why the measured photocurrents are weak.

There are several indications that we might have achieved electrical detection of SPPs in our device. We do observe a clear polarization dependence of the photocurrent signal when laser light impinges directly on the grating, as shown in Fig. 4. Also, the photocurrent signal can be significantly enhanced by applying a reverse bias to the diode itself as evidenced in Fig. 5.

However, on the basis of the results shown in Fig. 6, we cannot rule out the possibility that the photocurrent signal obtained at the position of the grating has the same origin as the photocurrent signal obtained directly from the silicon substrate.

The question remains as to the origin of the photocurrent from the substrate. One possible explanation is that this photoresponse is due to light scattering of the SiO_2-surface such that it directly hits the silicon mesa.

The photocurrent peaks originating from protrusions in the aluminum are, perhaps, the clearest indication for plasmonic excitations in our device. When the small aluminum domes are illuminated by laser light, SPPs with a broad range of wavevectors are generated and can travel along the aluminum–air interface up the mesa where they could either directly or indirectly via a photon scattering process excite electron–hole pairs in the active diode region that lead to a measurable photocurrent.

Phys. Status Solidi B **249**, No. 4 (2012)

777

Original

Paper

5 Conclusion If fully CMOS-compatible plasmonic interconnects can be realized, they could constitute a viable alternative to current metallic interconnects whose increasing delay times and power dissipation can be expected to be a major limiting factor in the performance increase of electrical systems within 10 years. The main question that we address with our experimental investigations is how optical excitation and electrical detection of SPPs can be realized in CMOS-compatible silicon pin-structures. To that end, we introduced a grating structure in the aluminum contact metallization of the vertical pin-diode and performed SPCM measurements. The aim was to excite SPPs at the interface between aluminum metallization and SiO_2 passivation that propagate towards the vertical double mesa pin-diode where they are detected via the generation of electron–hole pairs.

Since, we cannot separate signals from SPP excitations from other contributing effects with absolute certainty in our photocurrent measurements, further investigations are necessary in order to assess the suitability of all-silicon pin structures for electrical detection of SPPs. We are currently pursuing a number of possible improvements: by moving to Ge-based pin-diodes and selecting an excitation wavelength in the communication band (1550 nm), the direct creation of electron–hole pairs in the Si substrate can be avoided. The use of optimized grating coupler structures [20] in conjunction with waveguides that also confine the travelling plasmon in the plane, possibly also with enhanced propagation lengths, should allow boosting the conversion efficiency from incident photons to detectable current.

References

[1] International Technology Roadmap for Semiconductors, ITRS (2008).
[2] D. Miller, Proc. IEEE **97**, 1166 (2009).
[3] N. Engheta, Science **317**, 1698 (2007).
[4] N. Engheta, A. Salandrino, and A. Alu, Phys. Rev. Lett. **95**, 095504 (2005).
[5] A. Alu and N. Engheta, Phys. Rev. Lett. **103**, 143902 (2009).
[6] J. T. Kim, J. J. Ju, S. Park, M.-S. Kim, S. K. Park, and M.-H. Lee, Opt. Express **16**, 13133 (2008).
[7] W. L. Barnes, A. Dereux, and T. W. Ebbesen, Nature **424**, 824 (2003).
[8] J. A. Conway, S. Sahni, and T. Szkopek, Opt. Express **15**, 4474 (2007).
[9] C. Delacour, S. Blaize, P. Grosse, J. M. Fedeli, A. Bruyant, R. Salas-Montiel, G. Lerondel, and A. Chelnokov, Nano Lett. **10**, 2922 (2010).
[10] A. V. Krasavin and A. V. Zayats, Opt. Express **18**, 11791 (2010).
[11] S. Zhu, T. Y. Liow, G. Q. Lo, and D. L. Kwong, Appl. Phys. Lett. **98**, 021107 (2011).
[12] S. Zhu, T. Y. Liow, G. Q. Lo, and D. L. Kwong, Opt. Express **19**, 8888 (2011).
[13] R. J. Walters, R. V. A. van Loon, I. Brunets, J. Schmitz, and A. Polman, Nature Mater. **9**, 21 (2010).
[14] J. A. Dionne, K. Diest, L. A. Sweatlock, and H. A. Atwater, Nano Lett. **9**, 897 (2009).
[15] A. L. Falk, F. H. L. Koppens, C. L. Yu, K. Kang, N. de Leon Snapp, A. V. Akimov, M.-H. Jo, M. D. Lukin, and H. Park, Nature Phys. **5**, 475 (2009).
[16] K. Balasubramanian, M. Burghard, K. Kern, M. Scolari, and A. Mews, Nano Lett. **5**, 507 (2005).
[17] H. L. Offerhaus, B. van den Bergen, M. Escalante, F. B. Segerink, J. P. Korterink, and N. F. van Hulst, Nano Lett. **5**, 2144 (2005).
[18] I. H. Malitson, J. Opt. Soc. Am. **55**, 1205 (1965).
[19] A. G. Mathewson and H. P. Myers, Phys. Scr. **4**, 291 (1971).
[20] I. P. Radko, S. I. Bozhevolnyi, G. Brucoli, L. Martín-Moreno, F. J. García-Vidal, and A. Boltasseva, Phys. Rev. B **78**, 115115 (2008).